

Poly(aryleneethynylene)s with Orange, Yellow, Green, and Blue Solid-State Fluorescence

Yiqing Wang,[†] Jong Seung Park,[‡] Jake Peter Leech,[†] Shaobin Miao,[†] and Uwe H. F. Bunz^{*,†}

School of Chemistry and Biochemistry and School of Polymer, Textile and Fiber Engineering, Georgia Institute of Technology, Atlanta, Georgia 30332

Received December 6, 2006; Revised Manuscript Received January 23, 2007

ABSTRACT: Polyester side-chain grafted poly(aryleneethynylene)s (PEPAE) containing benzene and thiadiazole units were synthesized. Electrospinning allowed processing these PEPAEs into nanostructured materials. Large surface areas could be uniformly covered (100 cm²) by this technique. Side chain length, polymer concentration and solvent determined the type of nanostructure (nanofibers or microspheres) formed. When a polyester substituted poly(*p*-phenyleneethynylene) was electrospun into liquid nitrogen, a unique type of nanoporous morphology emerged.

Introduction

Conjugated polymers are organic semiconductors and as such they find wide use in sensory and device applications which include but are not restricted to light emitting diodes, thin film transistors and photovoltaic cells.^{1–3} Poly(aryleneethynylene)s (PAE) are an important subclass of this genre; they can be highly fluorescent, are chemically stable, and are easily synthesized by either the Heck–Cassar–Sonogashira coupling or by alkyne metathesis.^{4–8} PAEs have recently been used in advanced biodetection schemes,^{9–11} in light emitting diodes,^{12,13} and in transistor type applications.¹⁴ As a general matter, the photo-physical properties of PAEs are critically dependent upon chain ordering, conformation and selection of suitable aromatic building blocks.^{15–18} In this contribution we examine the influence of long grafted polyester side chains on the spectroscopic properties of electrospun preparations of PAEs that contain either only benzene units (poly(*p*-phenyleneethynylene), PPE) or a ternary benzothiadiazole-*co*-alkyne-*co*-benzene-*co*-alkyne (**9–12**) backbone.^{5a} Specifically, we compare the emissive properties of electrospun¹⁹ grafted PPE **5** and dioctyl-PPE **6**²⁰ and the PAEs **9–12**; the differences in morphology and in optical properties are significant.

Nanostructured and microstructured conjugated polymers are attractive, due to their (a) increased surface/bulk ratio and (b) their small features, potentially useful for photonic applications and enhanced sensing and device performance.^{21–25} We have investigated the structuring of PAEs by membrane casting²¹ and the use of breath figures.²² We demonstrate now that electrospinning¹⁹ is a viable method to micro and nanostructure PPEs. In the electrospinning process, a syringe pump feeds a concentrated polymer solution into a metallic nozzle.¹⁹ The metallic nozzle and therefore the polymer are under a large positive static voltage of 10–20 kV. The conducting counter surface (aluminum foil, indium tin oxide coated glass, etc.), the collector, is grounded. When the polymer solution is fed through the nozzle, the highly positively charged pendent “drop” of the polymer solution at the tip of the needle deforms into a Taylor cone by

the electrostatic repulsion in the polymer solution stemming from the high surface charges. In combination with the electrostatic attraction to the oppositely charged counter surface these forces overcome the surface tension of the droplet and a liquid jet emanates from the nozzle. During the spinning process the jet is stretched, thinned and whipped. The concomitant loss of solvent further thins the fiber, which is deposited as a mat of nonwoven material on the grounded counter surface, for example aluminum foil. The decrease in the diameter of the formed fiber during the spinning process is due to a bending instability associated with the electrified jet. The electrospinning process forms fibers with diameters that range from 20 nm to 1 μ m. In nonviscous solutions the formation of microspheres or beads is predominant under these conditions due to the varicose breakup of the electrified jet. Electrospinning is a relatively simple process and it allows coating macroscopic areas (10 cm \times 10 cm) with nanoscopic polymer features. Electrospinning has therefore advantages with respect to size and control when compared to other nanostructuring methods that are often only amenable to the structuring of small scale samples.

Results and Discussion

Synthesis. The investigated dioctyl-PPE **6** was prepared according to ref 20 and had a degree of polymerization (DP) of 60 and a polydispersity (M_w/M_n) of 2.9. The polyester-substituted PPE **5** was prepared according to Scheme 1. Starting from the diiodide **1**, the tin–bis(octanoate)-catalyzed reaction with caprolactone (**2**) furnished the precursor monomer **3** in quantitative yield. The monomer **3** was dissolved in THF, (Ph₃P)₂PdCl₂, CuI, piperidine, and acetylene gas were added^{5b} to give the soluble precursor polymer **4**, fully characterized by NMR and gel permeation chromatography (GPC). According to GPC, **4** had a DP of 60 and an M_w/M_n of 3.6. In a second step, tin bisoctanoate and 60 equiv of caprolactone were added to **4** and reacted for 4 h at 100 °C to give the polyester grafted polymer **5** with the assigned constitution.²⁶ Attempts to make the grafted aromatic diiodide first and then prepare the PPE failed, likely due to the intrinsically low concentration of the reactive aromatic iodides in the grafted species. NMR spectroscopy of **5** only shows the presence of the polyester side chains, due to the large difference in signal intensity between

* Corresponding author. E-mail: uwe.bunz@chemistry.gatech.edu.

[†] School of Chemistry, Georgia Institute of Technology.

[‡] School of Polymer, Textile and Fiber Engineering, Georgia Institute of Technology.

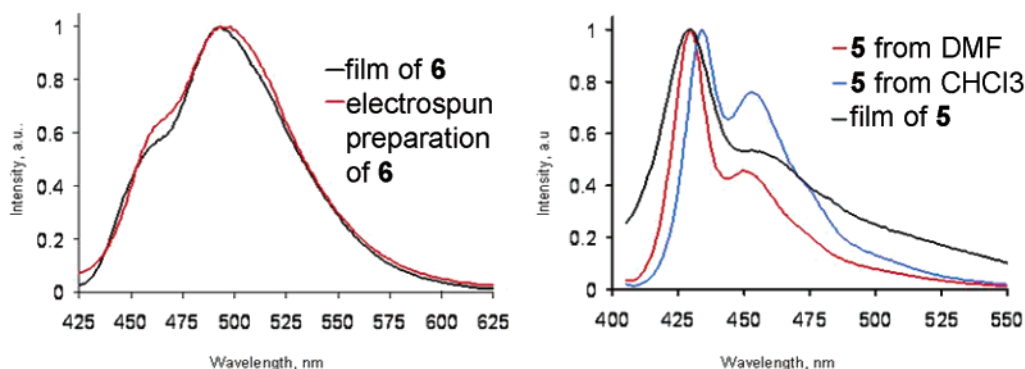
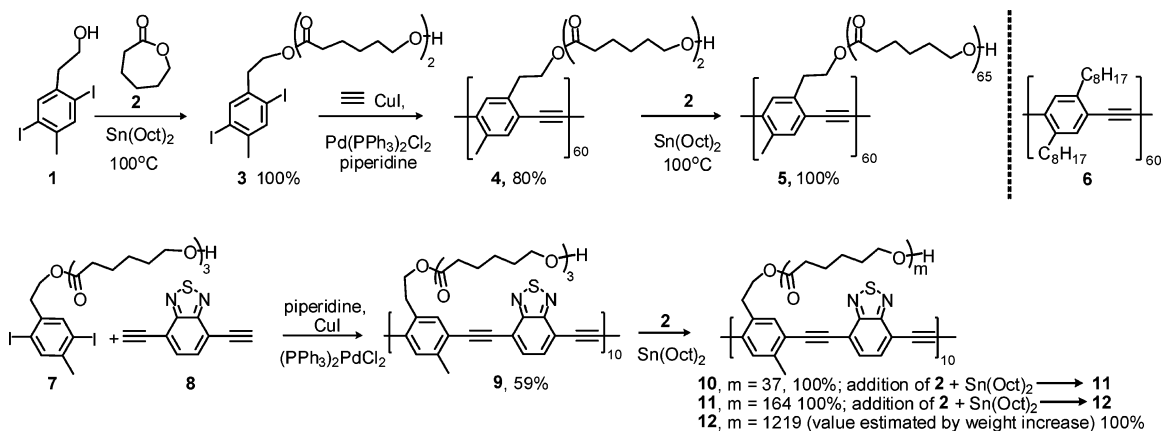


Figure 1. Left: Emission spectra of diethyl-PPE **6** as spin-cast film and as electrospun sample (λ_{max} film = 497 nm; λ_{max} microspheres 493 nm). Right: Emission spectra of polyester-PPE **5** as electrospun from DMF or from chloroform and as thin spin-cast film (λ_{max} DMF = 430 nm, progression = 1132 cm^{-1} ; λ_{max} Film = 430 nm; λ_{max} fiber CHCl_3 = 435 nm, vibronic progression = 1132 cm^{-1}).



Figure 2. Photograph of polymers **9–12** (left to right are **9**, **10**, **11**, and **12**) under UV irradiation.

Scheme 1. Synthesis of Polyester-g-PPE **5 and of the Polyester-g-PAEs **9–12****



side and main chains. The polymer **5** consists to over 99% of side chains and to less than 1% of the conjugated, fluorescent backbone.

Polymer **9** was synthesized by coupling of **7** to **8** in the presence of piperidine, CuI , and $(\text{PPh}_3)_2\text{PdCl}_2$ using THF as solvent (Scheme 1). After reacting for 24 h at room temperature, polymer **9** was obtained as a green, metallic-lustrous solid in 59% yield. The GPC measurement shows that **9** has an M_n of 6.6×10^3 with a PDI of 2.5, which corresponds to a DP of 10. The reaction of **9** with **2** furnishes **10**, which was isolated and then further reacted with **2** in the presence of tin octanoate to give **11**, while isolated **11** was reacted with **2** under identical conditions to give **12**. The polymers **10**, **11**, and **12** carry polyester side chains with 37, 1.6×10^2 , and 1.2×10^3 repeat units, respectively.

Optical Properties. Grafted polyester side chains reduce the interchain interactions between the PAE backbones.^{15–17} As a result, thin films of polymer **5** show an emission spectrum that is similar to that obtained for PPEs in chloroform solution. The formation of interchain excimerlike species is suppressed, and, the emission intensity of polymer **5** in solid state is much stronger than that of its precursor **4** or of diethyl PPE **6** (Figure 1). For the discussion of the optical properties of electrospun fibers of **5** see below. The trend of increasing solid-state fluorescence intensity was also observed in the polyester side chain substituted PAEs **9–12** (Figure 2). While **9** is practically nonfluorescent in thin films, **10** shows an increased but orange fluorescence with a λ_{max} at 541 nm. When going to **11** and **12** the fluorescence intensity increases and λ_{max} , both in the bulk as well in thin spin-cast films, blue-shifts to 511 nm. The graft

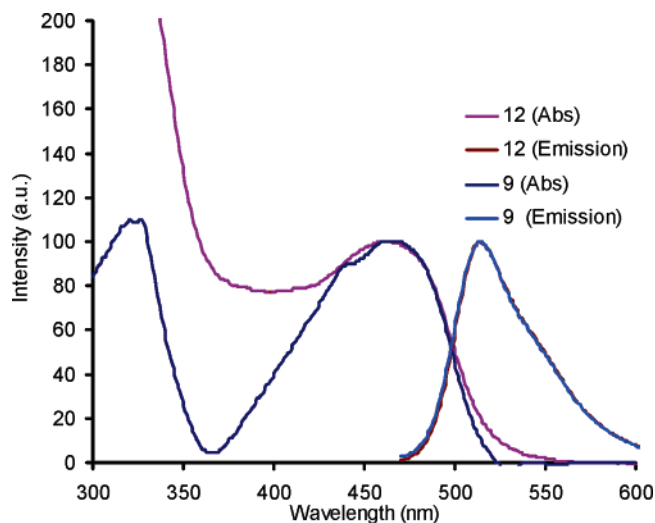


Figure 3. Normalized absorption and emission spectra for polymers **9** and **12** in CHCl_3 . The quantum yield for polymer **12** is 0.68 in CHCl_3 ; λ_{max} absorption solution = 468 nm, λ_{max} emission solution = 516 nm.

polymer **12** appears fibrous and is strongly yellow emitting with a greenish tinge. In chloroform solution, however, the absorption and emission spectra of **9–12** are identical to each other and their fluorescence quantum yields are very similar ($\Phi_9 = 0.59$, $\Phi_{10} = 0.65$, $\Phi_{11} = 0.62$, $\Phi_{12} = 0.69$). The quantum yields of **5** $\Phi_5 = 0.86$ while that of **6** is close to unity and literature described.⁴ In the solid state (thin film) the absorption spectra of **9–12** are consecutively blue-shifted with $\lambda_9 = 525$ nm, $\lambda_{10} = 485$ nm, $\lambda_{11} = 480$ nm, and $\lambda_{12} = 465$ nm resulting. Solid state absorption and emission are influenced by the increased length of the attached polyester chains, due to the decrease in interchain interactions and possibly also due to a conformational effect. PAE backbones with longer polyester side chains probably show a larger torsion of the arene units with respect to each other.²⁶ From Figure 2 it is gleaned that the solid-state emission of **9** in substance is very low, probably due to the formation of nonfluorescent aggregates. In **10–12** these aggregates form less and single chain fluorescence is observed in **12**.

The emission of **9–12** in the solid state can be shifted continuously from 560 to 510 nm, depending upon the length of the grafted polyester side chains. The solid-state emission spectra of **9–12** are broad and featureless and do not show any vibronic coupling. If “diluted” appropriately by polyester-grafted side chains, these PAE-backbones are brightly fluorescent in the solid state. In the polymer **12** the concentration of the fluorophore is less than 0.2 wt %, yet the material is most emissive. The corresponding dialkyl and dialkoxy PAEs containing benzothiadiazoles are nonfluorescent green-metallic lustrous solids as a consequence of aggregate formation.⁵

Electrospinning. In a first experiment we electrospun dioctyl-PPE **6** from chloroform. Microspheres with an average diameter of 1–1.5 μm formed (Figure 5). If we electrospun solutions of **6** from THF, benzene, or toluene, we did not obtain any structured materials. From these experiments, we conclude that dioctyl-PPE **6** undergoes an electrospinning process. However, the formed microspheres are interesting in their own right. In Figure 8, a macroscopic sample of electrospayed **6** on a piece of aluminum foil is shown. Its fluorescence is green ($\lambda_{\text{max}} = 497$ nm). Thin films of **6** show a similar but more blue-shifted emission with a λ_{max} emission of 493 nm (Figure 1). Is the formation of microspheres from **6** surprising? Electrospun fibers

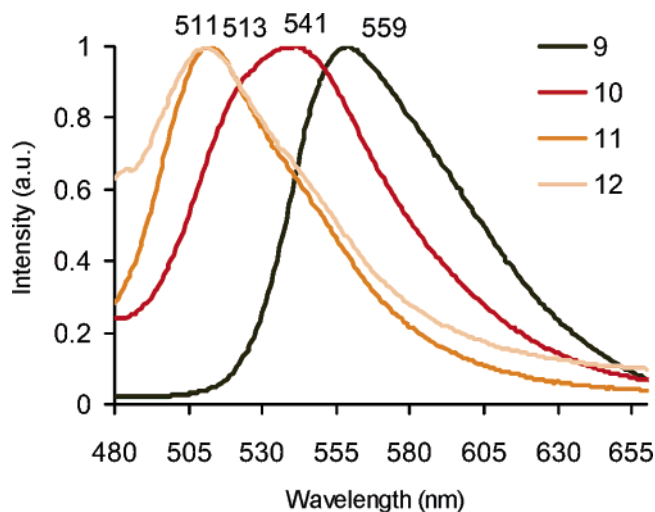


Figure 4. Normalized thin film (spin-cast from chloroform) emission spectra of polymers **9–12**.

are formed from a wide variety of polymers that form viscous solutions.¹⁹

Concentrated solutions of dialkyl-PPEs, such as **6**, form fragile gels in aromatic solvents or chloroform. These gels easily break up under mechanical stress and give rise to solutions of low viscosity.²⁷ The formation of microspheres during electrospinning, or better electrospaying, is therefore not too surprising.²⁸

The length of the side chain graft is an important factor in the quality of the electrospun fiber preparation. Polymers **9** and **10**, which carry 3 and 37 repeat units of polyester side chains respectively, do not form fibers when electrospayed, but microspheres. However, polymers **11** and **12**, which bear polyester side chains with more than 1.6×10^2 and 1.2×10^3 repeat units, form finely spindled and interconnected nanoscale fibers (Figure 6c,d). Viscosity is an important issue that determines the ratio of droplets vs fibers. The higher the viscosity of a specific solution is, the better is the process of fiber formation. Figure 7 shows the concentration-dependent development of the morphology of a solution of **11** in chloroform when electrospinning. Solutions with 2.5 and 5 wt % of polymer are not particularly viscous and form mobile liquids. These materials electrospay instead of electrospin. However, when the concentration of **11** is above 10%, we can obtain nicely developed fibrous preparations (Figure 7 right) with only a very few microspheres present.

When a solution of **5** is electrospayed from DMF (Figure 9), 1–2 μm sized spheres and some smallish fibers form. However, upon electrospinning **5** from chloroform, well-defined fibers with diameters ranging from 50 nm to 1 μm form (Figure 9 middle, right). The chloroform electrospun fibers of **5** cast a uniform mat of nonwoven fabric on the aluminum foil. These nonwoven fibers are bright blue luminescent (Figure 8, right) and exhibit an emission maximum that is (Figure 1) 5 nm red-shifted from that of the thin films and the microspheres electrospayed from DMF. Additionally, the vibronic fine structure is stronger developed in the electrospun fibers; the differences between thin film and nanofiber preparations, even though subtle, are possibly due to nanoconfinement and chain orientation effects that could change both interchain interactions as well as planarization of the chains (Figure 1).^{15–18} Figure 8 shows that upon the correct choice of backbone and side chains PAEs can form highly fluorescent preparations that range in

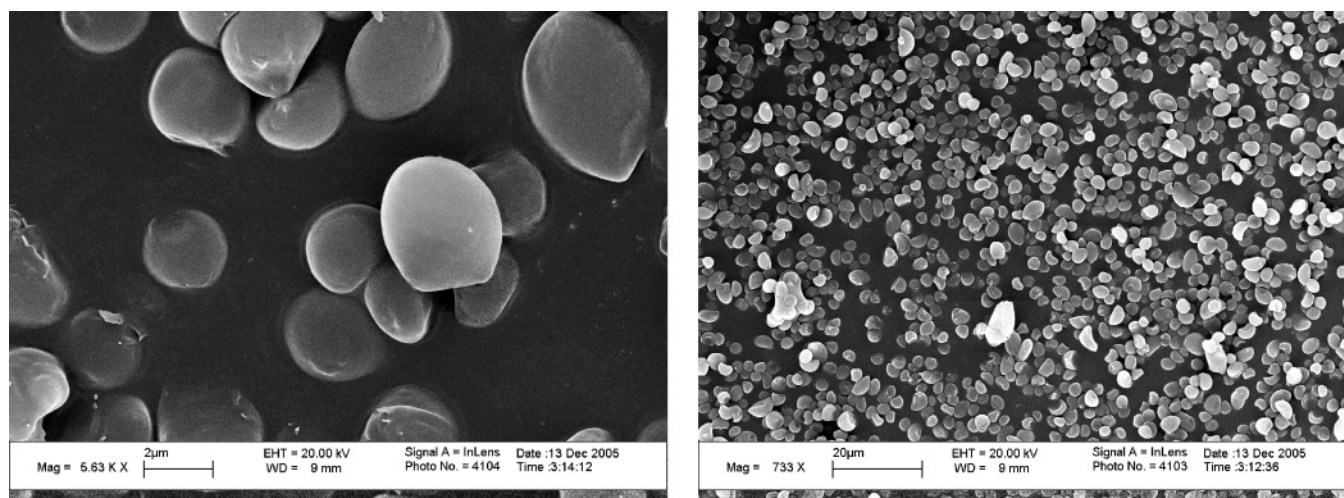


Figure 5. Scanning electron micrograph of electrospayed preparations of dioctyl-PPE **6** from chloroform. Spheres are 1–2 μm in diameter.

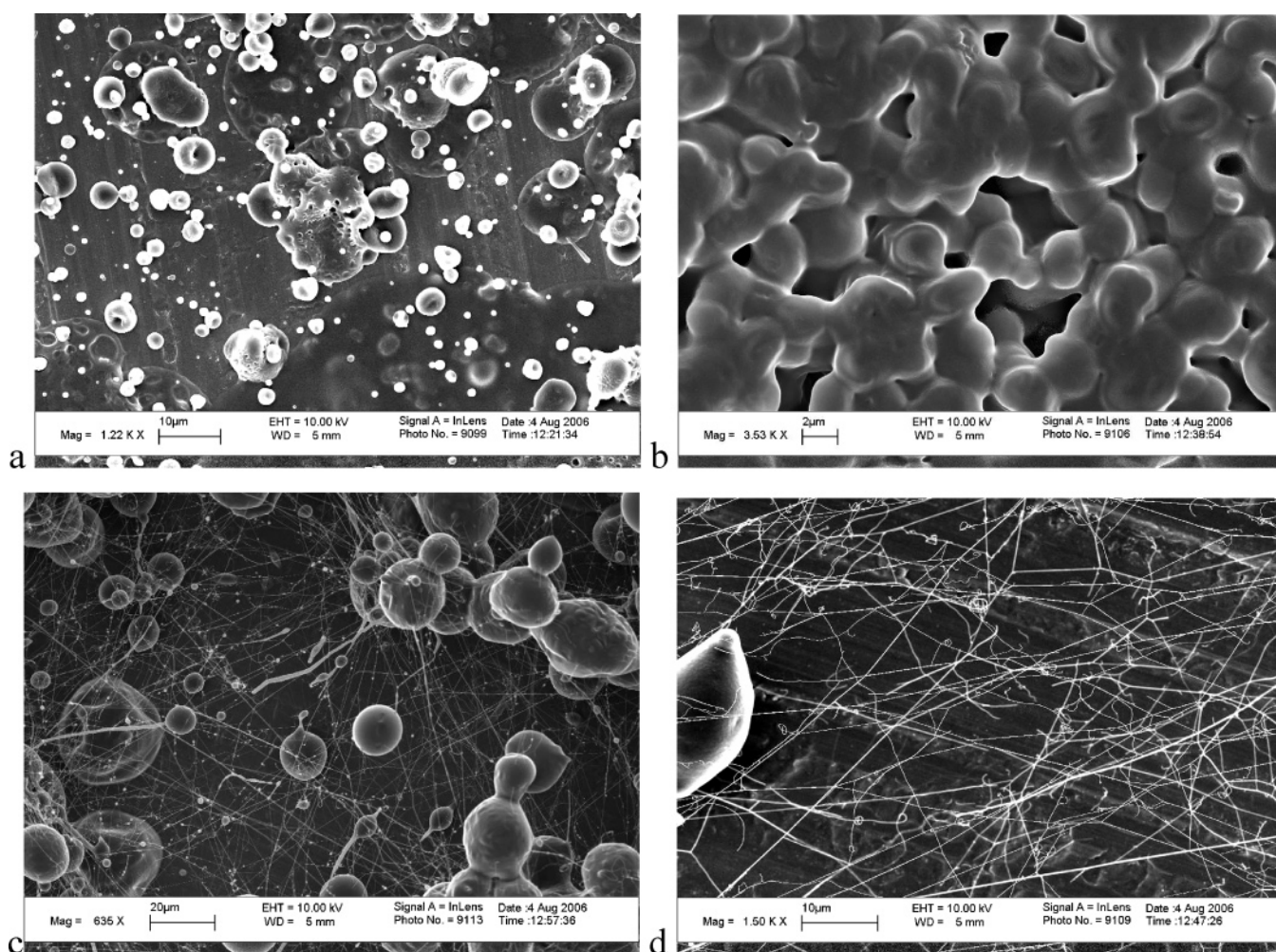


Figure 6. Scanning electron micrograph of electrospun preparations of polymer **9** (a), **10** (b), **11** (c), and **12** (d). All experiments were done at 10 wt % solution in chloroform.

emission color from red to blue, by combining two different backbones with suitable, nonconjugated polyester grafts.

All of the electrospun/electrospayed and microstructured preparations are hydrophobic and display static contact angles that range from 120 to 150° (Figure 10). Thin films of **6** show a contact angle of 100°, while the electrospun microspheres have an increased contact angle of 149°. In the case of the polyester-PPE **5**, the thin film contact angle is only 83° due to the hydrophilicity conferred by the polyester side chains. Here,

the contact angle of the microstructured material is 121° for the fibers and 140° for the microspheres. The contact angle of the used aluminum foil was determined as a control and is 65(±2)°.

What determines the contact angle? According to Cassie's law

$$\cos \Theta = X_1 \cos \Theta_1 + (1 - X_1) \cos \Theta_2$$

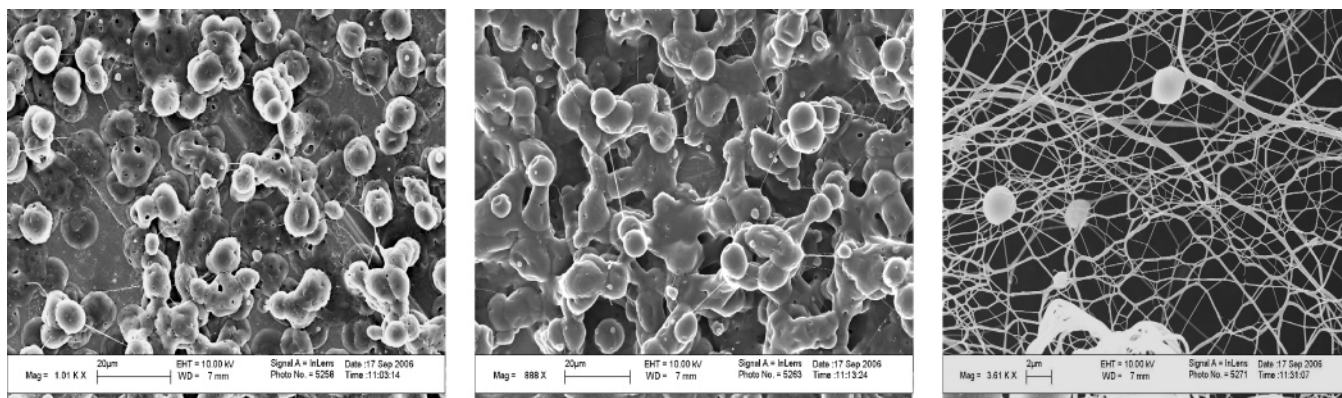


Figure 7. Scanning electron micrograph of electrospun preparations of polymer **11** dissolved in chloroform. Solutions contain 2.5 wt % (left), 5 wt % (center), and 10% (right).

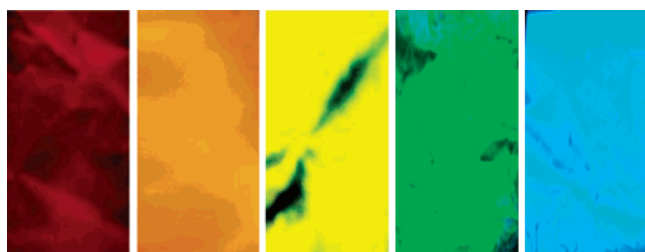


Figure 8. Macroscopic electrospun preparations (from left or right) of **10**, **11**, **12**, dioctyl-PPE **6**, and polyester-PPE **5** on aluminum foil. The pieces are approximately 1.5 cm \times 4 cm. The samples were obtained by electrospinning a 10 wt % solution of polymer in chloroform.

the cosine of a contact angle Θ_1 of a composite surface with water or any other solvent is the sum of the cosines of their respective specific contact angles Θ_1 and Θ_2 multiplied by their surface fractions X_1 and $(1 - X_1)$.²⁹ The contact angle of air and water is 180° and the equation simplifies to

$$\cos \Theta = X_1(\cos \Theta_1 + 1) - 1$$

If the surface fraction of the polymer, X_1 , is zero, then the contact angle will be 180°, as in the air–water contact angle. Cassie's law does not take into account the shape of the surface. Only the surface fraction that is covered and the specific contact angle play a role. We can exclude any influence of the aluminum foil on the observed contact angle, as we use thick films for the surface wetting experiments. Additionally, we would expect a decrease in the contact angle if the interface of the aluminum foil and the polymer would be important. We conclude that the surface coverage is higher for the fibers than for the microspheres. The absolute surface coverage is difficult to determine from the SEM pictures, so we cannot exclude a shape effect for the contact angle.

Very recently, Xia et al. described the electrospinning of polystyrene solutions into a liquid nitrogen filled conducting receiver.³⁰ They reported thin electrospun polystyrene fibers that were porous. We attempted the electrospinning process with **5** under similar conditions, but instead of fibers we found nanoporous morphologies. Figure 11 shows the SEM pictures obtained from a representative example of **5**. The coverage of the aluminum foil is not uniform but spots of materials are observed. Under larger magnification one can see that the material has a spongelike quality. The emission spectrum of this material shows a λ_{max} of 432 nm, i.e., intermediate between that of the nanofibers and that of the microspheres. We speculate that the spongelike morphology arises upon the fast cooling of the electrosprayed/spun solution of **5** and the consecutive rapid evaporation of the liquid nitrogen.

Conclusions

Polyester side-chain substituted PPEs **5**, **11**, and **12** can be electrospun to give nonwoven, nanofibrous morphologies. The correct choices of concentration (high) and solvent (chloroform) are critical. When DMF is used, hairy microspheres formed instead of fibers. When dioctyl-PPE **6** was electrosprayed, microspheres formed and none of the fibers were observed. The occurrence of microspheres vs nanofibers or electrospraying vs electrospinning is determined by the viscosity of the solution.^{19,27} The high molecular weight of grafted polymers **5**, **11**, and **12** makes their solutions in chloroform viscous, ideal for electrospinning. If the electrospinning of grafted PPE is performed into liquid nitrogen, spongelike morphologies are obtained but not fibers.

The emission of the electrospun fibers of **5** is somewhat red-shifted but sharp with a well developed vibronic progression. The dioctyl-PPE **6** is yellow in appearance and green emissive, while **5** is colorless, appears white and blue emissive, despite

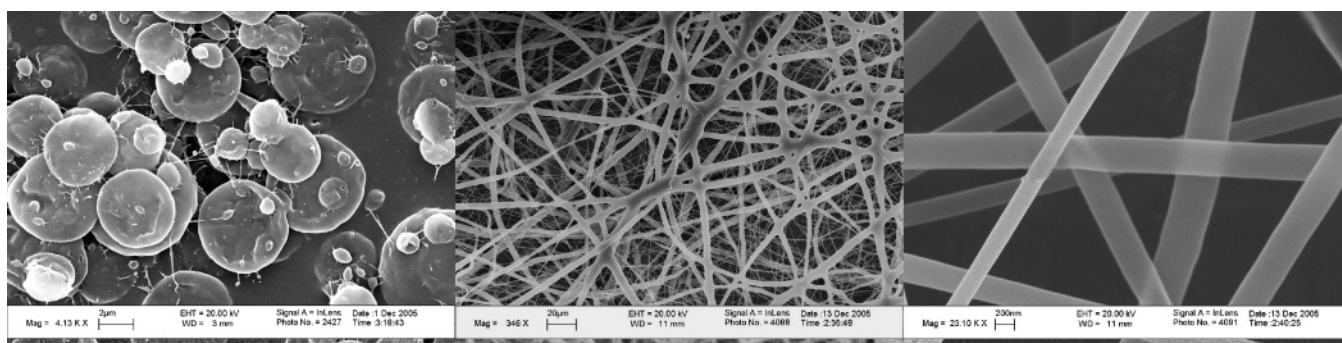


Figure 9. Scanning electron micrographs of samples of polymer solutions of **5** electrospun from DMF (left) and from chloroform (middle, right).



Figure 10. Contact angle of water on preparations of **5** electrospun from DMF (left, 140°), **5** electrospun from chloroform (middle, 121°), and **6** electrospun from chloroform (right, 149°).

their identical chemical backbones. In **5**, **11**, and **12** the long polyester chains ensconce the polymer backbone and act both as an insulator against interchain interactions, which normally lead to excimer-type behavior,^{15a} as well suppress planarization.^{15b} While **9** is nonfluorescent, **10–12** are highly emissive in the solid state. Electrospun/electrosprayed films of **5** and **6** can be annealed with a heat gun to give large scale optically clear, thin films on conducting and semiconducting surfaces without the need for spin-casting. Other applications of electrospun/electrosprayed films might include water repellent fluorescent coatings for diverse sensory applications.

Experimental Section

Macromonomer 3. 1 (540 mg, 1.40 mmol), ϵ -caprolactone (319 mg, 2.80 mmol), and tin(II) 2-ethylhexanoate (1 mg, 3 μ mol) were placed under nitrogen into an oven-dried Schlenk flask equipped with a stirring bar. The mixture was heated to 100 °C, and allowed to react for 12 h. After being dried under vacuum at 60 °C overnight, the diiodopolyester macromonomer **3** was obtained as a colorless solid without further workup (859 mg, 100%). GPC (vs polystyrene standards in chloroform): $M_n = 620$, $M_w/M_n = 1.1$. IR (KBr, cm^{-1}): ν 2941, 2893, 2866, 1722, 1683, 1652, 1506, 1471, 1456, 1394, 1294, 1244, 1190, 1107, 1045, 962, 933, 877, 840, 731, 709. ^1H NMR (CDCl_3 , 400 MHz): $\delta = 7.67$ (s, 1H), 7.63 (s, 1H), 4.24 (t, 2H), 4.05 (t, 2H), 3.64 (t, 2H), 2.98 (t, 2H), 2.48 (s, 3H), 2.30 (t, 4H), 1.68–1.30 (m, 12H). ^{13}C NMR (CDCl_3 , 400 MHz): $\delta = 173.73$, 173.54, 173.29, 141.91, 139.91, 139.87, 139.82, 100.76, 100.03, 64.54, 64.14, 63.95, 63.10, 62.62, 38.64, 34.23, 34.12, 33.95, 33.82, 33.34, 28.53, 28.35, 28.18, 26.96, 25.93, 25.53, 25.31, 24.98, 34.69, 24.58, 24.39.

Macromonomer 7 was synthesized using the same procedure as **3**. Characterization is identical. GPC (vs polystyrene standards in chloroform): $M_n = 730$, $M_w/M_n = 1.1$.

Polymer 4. 3 (859 mg, 1.40 mmol) was combined with piperidine (1.5 mL), THF (1.5 mL), $(\text{PPh}_3)_2\text{PdCl}_2$ (2 mg, 2 μ mol, 0.2 mol %), and CuI (1 mg, 5 μ mol, 0.4 mol %) in a Schlenk flask of known volume (37 mL). Acetylene gas^{5b} (34 mL, 1.40 mmol)

was added through the purged side arm with a balloon. The mixture was allowed to stir at room temperature for 24 h and was then extracted with dichloromethane (50 mL). The organic layer was washed with ammonium hydroxide (10%, 2 \times 50 mL) and HCl (10%, 50 mL). The organic layer was dried over MgSO_4 and concentrated under reduced pressure. The remaining mixture (10 mL) was precipitated into acidified methanol. The polymer was collected over a fritted funnel, and purified by being redissolved in dichloromethane and reprecipitated into acidified methanol. A greenish yellow polymer, **4** (0.434 g, 81%) was obtained. GPC (vs polystyrene standard in chloroform): $M_n = 2.3 \times 10^4$, DP = 60, $M_w/M_n = 3.6$. ^1H NMR (400 MHz, CDCl_3): $\delta = 7.41$ (bs), 4.04 (bt), 3.62 (bt), 3.49 (s), 2.76 (bs), 2.32–2.28 (bt), 1.62–1.40 (bm), 1.36–0.90 (bm). ^{13}C NMR (400 MHz, CDCl_3): $\delta = 173.69$, 141.01, 133.35, 123.85, 123.18, 93.46, 92.54, 65.15, 64.09, 63.05, 62.55, 40.28, 38.56, 34.06, 32.27, 28.804, 28.29, 25.47, 23.10, 25.25, 24.52, 20.29, 14.10, 10.83.

Polymer 5. 4 (405 mg, 1.05 mmol, based on 386 g mol^{-1} per repeat unit), ϵ -caprolactone (11.4 g, 0.100 mol), and tin(II) 2-ethylhexanoate (1 mg, 3 μ mol) were added into an oven-dried Schlenk flask with stirring. The flask was charged with nitrogen and then heated up to 100 °C. After 4 h, the reaction mixture had solidified. The solid was dissolved in hot chloroform and precipitated from acidified methanol. After drying under oil pump vacuum at 60 °C overnight, polymer **6** (4.841 g, 100%) was obtained as a bright yellowish-green solid. GPC (vs polystyrene standard in chloroform): $M_n = 4.6 \times 10^5$, $M_w/M_n = 3.1$. Repeat = 7617 g mol^{-1} , DP = 60 (main chain), $P_m = 65$ (side chain). IR: 2941, 2864, 1718, 1419, 1363, 1292, 1238, 1174, 1047, 960, 933, 840, 732, 709. ^1H NMR (400 MHz, CDCl_3): 4.04 (bm), 2.28 (bm), 1.62 (bm), 1.36 (bm). ^{13}C NMR (400 MHz, CDCl_3): $\delta = 173.50$, 64.34, 34.34, 32.27, 28.56, 25.73, 24.52. Calcd for $\text{C}_{24360}\text{H}_{39600}\text{O}_{7860}\text{I}_2$, C 63.81, H 8.71; Found: C 62.96, H 8.69.

Polymer 9. 7 (1.46 g, 2.00 mmol), **8** (0.372 g, 2.00 mmol),^{5a} piperidine (1.5 mL), THF (1.5 mL), $(\text{PPh}_3)_2\text{PdCl}_2$ (2.0 mg, 2.8 μ mol) and CuI (1.0 mg, 5.3 μ mol) were combined in a Schlenk flask and degassed and stirred at room temperature for 24 h. The resulting polymer was extracted with dichloromethane (50 mL), washed with 10% ammonia (50 mL \times 2) and 10% hydrochloric acid (50 mL). The solvent was removed under reduced pressure. The crude product was repeatedly dissolved in dichloromethane (10 mL), filtered and precipitated into methanol (2 \times). A metallic green polymer was obtained (0.804 g, 61%). GPC (vs polystyrene standard in chloroform): $M_n = 6.6 \times 10^3$ (vs polystyrene standards). Repeat = 659 g mol^{-1} , DP = 10, $M_w/M_n = 2.5$. IR (KBr, cm^{-1}): ν 3427, 3018, 2929, 2856, 1720, 1643, 1519, 1421, 1215, 1029, 927, 754, 669. ^1H NMR (400 MHz, CDCl_3): δ 7.75–7.50 (bs, 2H), 7.43–7.26 (bm, 2H), 4.46 (bs, 2H), 4.04 (bt, 4H), 3.62 (bs, 2H), 2.94 (bs, 2H), 2.28 (bt, 9H), 1.62 (bm, 12H), 1.36 (bm, 6H).

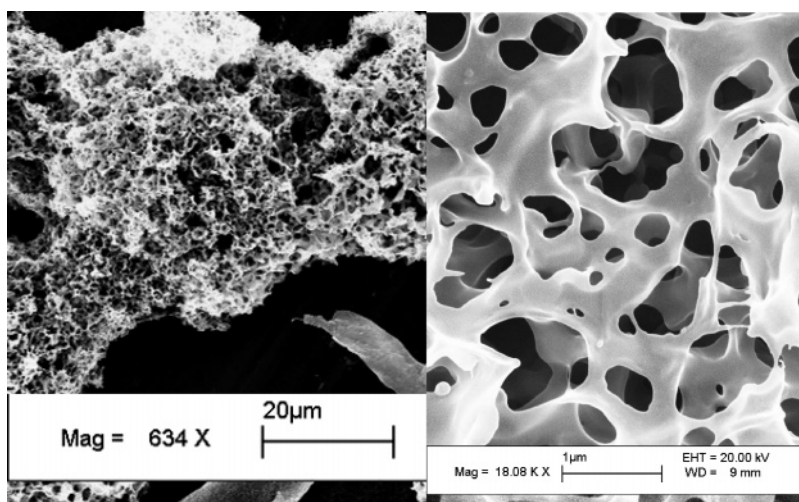


Figure 11. Scanning electron micrographs of samples of an electrospun preparation of **5**. The material was dissolved in chloroform and spun into liquid nitrogen. On the right-hand side the spongelike character of the morphology is visible.

^{13}C NMR (400 MHz, CDCl_3): δ 173.69, 173.50, 154.26, 140.72, 140, 40, 139.08, 137.09, 137.76, 132.80, 132.06, 122.06, 116.93, 96.22, 90.95, 64, 05, 62.45, 34.12, 34.02, 32.20, 28.23, 25.47, 25.25, 24.52, 20.29. Anal. Calcd for $\text{C}_{368}\text{H}_{440}\text{I}_2\text{N}_{20}\text{O}_{70}\text{S}_{10}$: C, 64.64; H 6.49; Found: C, 65.38; H, 6.20.

General Synthesis of Polymers 10, 11, and 12. A 100 mg sample of polycaprolactone-g-PAE (**9**, **10**, or **11**) was dried under oil pump vacuum at 70 °C before adding into 2 mL of caprolactone. The mixture was heated up to 110 °C until the polymer had dissolved, and then tin(II) 2-ethylhexanoate (1 mg, 3 μmol) was added. The reaction was heated to 110 °C and stopped after the mixture turned solid. The product was dissolved in chloroform, precipitated into methanol, collected on a fritted funnel, and dried under oil pump vacuum.

Polymer 10. 9 (100 mg) was added to caprolactone (2 mL) and tin(II) 2-ethylhexanoate (1 mg, 3 μmol) and reacted under standard conditions. A red polymer, **10** (1.10 g), was obtained. GPC (vs polystyrene standard in chloroform): $M_n = 45 \times 10^3$ (vs polystyrene standards). Repeat = 4.5×10^3 g mol^{-1} , DP = 10, $M_w/M_n = 2.4$, side chain length $m_{10} = 37$. IR: 2941, 2864, 1718, 1419, 1363, 1292, 1238, 1174, 1047, 960, 933, 840, 732, 709. ^1H NMR (400 MHz, CDCl_3): 7.75–7.20 (bm), 4.04 (bt), 3.62 (bs), 2.94 (bs), 2.28 (bt), 1.62 (bm), 1.36 (bm). ^{13}C NMR (400 MHz, CDCl_3): 173.69, 173.50, 65.15, 64.09, 63.05, 62.55, 34.06, 32.27, 28.29, 25.47, 25.25, 24.52, 20.29. Anal. Calcd for $\text{C}_{2408}\text{H}_{3840}\text{I}_2\text{N}_{20}\text{O}_{750}\text{S}_{10}$: C, 63.36; H, 8.48. Found: C, 62.57; H, 8.48.

Polymer 11. 10 (100 mg) was added to caprolactone (2 mL) and tin(II) 2-ethylhexanoate (1 mg, 3 μmol) and reacted under standard conditions. An orange polymer, **11** (0.872 g), was obtained. GPC (vs polystyrene standard in chloroform): $M_n = 19 \times 10^4$ (vs polystyrene standards). Repeat = 19×10^3 g mol^{-1} , DP = 10, $M_w/M_n = 2.4$, side chain length $m_{11} = 164$. IR: 2941, 2864, 1718, 1419, 1363, 1292, 1238, 1174, 1047, 960, 933, 840, 732, 709. ^1H NMR (400 MHz, CDCl_3): 4.04 (bt), 3.62 (bs), 2.28 (bt), 1.62 (bm), 1.36 (bm). ^{13}C NMR (400 MHz, CDCl_3): δ = 173.69, 173.50, 65.15, 64.09, 63.05, 62.55, 34.06, 32.27, 28.29, 25.47, 25.25, 24.52, 20.29. Anal. Calcd for $\text{C}_{10028}\text{H}_{16540}\text{I}_2\text{N}_{20}\text{O}_{3290}\text{S}_{10}$: C, 63.19; H, 8.75. Found: C, 62.36; H, 8.71.

Polymer 12. 11 (100 mg) was added to caprolactone (2 mL) and tin(II) 2-ethylhexanoate (1 mg, 3 μmol) and reacted under standard conditions. A colorless polymer, **12** (0.731 g), was obtained. GPC (vs polystyrene standard in chloroform): $M_n > 5 \times 10^5$ (over the detection limit), side chain length $m_{12} = 1.2 \times 10^3$ (estimated by weight increase). IR: 2941, 2864, 1718, 1419, 1363, 1292, 1238, 1174, 1047, 960, 933, 840, 733, 710. ^1H NMR (400 MHz, CDCl_3): 4.04 (bt), 3.62 (bs), 2.28 (bt), 1.62 (bm), 1.36 (bm). ^{13}C NMR (400 MHz, CDCl_3): 173.69, 173.50, 65.15, 64.09, 63.05, 62.55, 34.06, 32.27, 28.29, 25.47, 25.25, 24.52, 20.29. Anal. Calcd for $\text{C}_{2408}\text{H}_{3840}\text{I}_2\text{N}_{20}\text{O}_{750}\text{S}_{10}$: C, 62.83; H, 8.89. Found: C, 62.41; H, 8.78.

Electrospinning Procedure. Polymer solutions were prepared at a concentration of 10 wt % in various organic solvents (THF, DMF, chloroform, etc.). These solutions were transferred into the injection syringe (diameter 4.7 mm) and allowed to stand overnight to remove any trapped air inside the solutions. The electrospinning setup was followed according to previous reports.^{19,30,31} The polymer solution was pumped through a syringe needle (22 G), which was connected with a variable high voltage power supply (purchased from Glass High Voltage Inc.), at the speed of 0.2 mLh⁻¹. Fibers were collected on the conducting substrate itself, or a glass slides placed on top of the metal cathode, i.e., the aluminum foil. The distance between the tip of the syringe and the aluminum foil was fixed at 30 cm, and the applied voltages were 20 kV. The samples were investigated by SEM.

Scanning Electron Microscopy. Samples were cut out of the aluminum foil on which they were deposited, and attached by carbon tape to standard aluminum SEM stubs. The samples were sputter-coated with gold. The SEM used was a LEO 1530 thermally-assisted field emission scanning electron microscope, at 10 keV through the In-Lens detector.

Characterization. The ^1H and ^{13}C NMR spectra were measured on a Varian 300 MHz spectrometer or on a Bruker 400 MHz spectrometer using a broadband probe. IR data were collected by an FTIR-8400S infrared spectrophotometer (Shimadzu). The emission spectra were obtained on an RF-5301 PC Spectrofluorophotometer (Shimadzu). GPC measurements were conducted in chloroform (25 °C) with a SCL-10A VP UV-vis detector (Shimadzu). The molecular weights were determined vs polystyrene standards.

Quantum Yields. All absorption spectra were collected using a Shimadzu UV-2401PC spectrophotometer. All emission spectra were acquired using a Shimadzu RF-5301PC spectrofluorophotometer. The fluorescence quantum yields were determined using quinine sulfate (10^{-6} M in 0.1 M H_2SO_4 , $\Phi = 0.54$). All solutions were purged with nitrogen prior to measurement) using standard procedures according to ref 32. The quantum yields of **9–11** were determined by comparing the fluorescence emission intensities of equimolar solutions of **9–11** with the intensity obtained for **12**. Because both the spectral shape and the spectral shift for **9–12** in chloroform are identical, this type of measurement is reliable.

Acknowledgment. U.B. and J.P. thank the Department of Energy (DE-FG02-04ER46141). U.B., S.M., and Y.W. thank the NSF (CHE 0138659). We thank Prof. Mohan Srinivasarao and his graduate student Matije Crne for help in preparation of eletrosun samples of **9–12**, and Bradley Carson for revising this manuscript. We highly appreciate Dr. X. Zheng and Prof. M. Weck (School of Chemistry of Biochemistry, Georgia Institute of Technology) for the provision of elemental analyses of polymers **5** and **9–12**.

Supporting Information Available: A figure showing solution absorption spectra of **9–12** in chloroform. This material is available free of charge via the Internet at <http://pubs.acs.org>.

References and Notes

- (1) (a) Wegner, G.; Müllen, K. Eds.; *Electronic Materials: The Oligomer Approach*; Wiley-VCH: Weinheim, Germany, 1996. (b) Müllen, K.; Scherf, U. Eds.; *Organic Light Emitting Devices*; Wiley-VCH, Weinheim, Germany, 2006. (c) Kraft, A.; Grimsdale, A. C.; Holmes, A. B. *Angew. Chem.* **1998**, *37*, 402. (d) Bäuerle, P.; Mitschke, U. *J. Mater. Chem.* **2000**, *10*, 1471.
- (2) (a) Dimitrakopoulos, C. D.; Malenfant, P. R. L. *Adv. Mater.* **2002**, *14*, 99. (b) McCulloch, R. D. *Adv. Mater.* **1998**, *10*, 93.
- (3) (a) Mwaure, J. K.; Pinto, M. R.; Witker, D.; Ananthakrishnan, N.; Schanze, K. S.; Reynolds, J. R. *Langmuir* **2005**, *21*, 10119. (b) Yu, G.; Gao, J.; Hummelen, J. C.; Wudl, F.; Heeger, A. J. *Science* **1995**, *270*, 1789. (c) Shirota, Y. *J. Mater. Chem.* **2000**, *10*, 1.
- (4) (a) Bunz, U. H. F. *Adv. Polym. Sci.* **2005**, *177*, 1. (b) Bunz, U. H. F. *Acc. Chem. Res.* **2001**, *34*, 998. (c) Bunz, U. H. F. *Chem. Rev.* **2000**, *100*, 1605.
- (5) (a) Banguayo, C. G.; Evans, U.; Myrick, M. L.; Bunz, U. H. F. *Macromolecules* **2001**, *34*, 7592. (b) Wilson, J. N.; Waybright, S. M.; McAlpine, K.; Bunz, U. H. F. *Macromolecules* **2002**, *35*, 3799.
- (6) Zhao, X. Y.; Pinto, M. R.; Hardison, L. M.; Mwaure, J.; Muller, J.; Jiang, H.; Witker, D.; Kleiman, V. D.; Reynolds, J. R.; Schanze, K. S. *Macromolecules* **2006**, *39*, 6355.
- (7) See in the issue about poly(aryleneethynylene)s: Weder, C. *Adv. Polym. Sci.* **2005**, *177*.
- (8) Negishi, E.; Anastasia, L. *Chem. Rev.* **2003**, *103*, 1979.
- (9) (a) Wilson, J. N.; Wang, Y. Q.; Lavigne, J. J.; Bunz, U. H. F. *Chem. Commun.* **2003**, 1626. (b) Kim, I. B.; Erdogan, B.; Wilson, J. N.; Bunz, U. H. F. *Chem.—Eur. J.* **2004**, *10*, 6247–6254. (c) Kim, I. B.; Wilson, J. N.; Bunz, U. H. F. *Chem. Commun.* **2005**, 1273.
- (10) Disney, M. D.; Zheng, J.; Swager, T. M.; Seeberger, P. H. *J. Am. Chem. Soc.* **2004**, *126*, 13343.
- (11) DiCesare, N.; Pinto, M. R.; Schanze, K. S.; Lakowicz, J. R. *Langmuir* **2002**, *18*, 7785–7787.
- (12) Pschirer, N. G.; Miteva, T.; Evans, U.; Roberts, R. S.; Marshall, A. R.; Neher, D.; Myrick, M. L.; Bunz, U. H. F. *Chem. Mater.* **2001**, *13*, 2691.
- (13) (a) Schmitz, C.; Posch, P.; Thelakkar, M.; Schmidt, H. W.; Montali, A.; Feldman, K.; Smith, P.; Weder, C. *Adv. Funct. Mater.* **2001**, *11*, 41. (b) Breen, C. A.; Tischler, J. R.; Bulovic, V.; Swager, T. M. *Adv. Mater.* **2005**, *17*, 1981.

- (14) Xu, Y.; Berger, P. R.; Wilson, J. N.; Bunz, U. H. F. *Appl. Phys. Lett.* **2004**, *85*, 4219.
- (15) (a) Bunz, U. H. F.; Imhof, J. M.; Bly, R. K.; Bangcuyo, C. G.; Rozanski, L.; VandenBout, D. A. *Macromolecules* **2005**, *38*, 5892. (b) Miteva, T.; Palmer, L.; Kloppenburg, L.; Neher, D.; Bunz, U. H. F. *Macromolecules* **2000**, *33*, 652.
- (16) Halkyard, C. E.; Rampey, M. E.; Kloppenburg, L.; Studer-Martinez, S. L.; Bunz, U. H. F. *Macromolecules* **1998**, *31*, 8655.
- (17) Kim, J.; Swager, T. M. *Nature (London)* **2001**, *411*, 1030.
- (18) Haskins-Glusac, K.; Pinto, M. R.; Tan, C. Y.; Schanze, K. S. *J. Am. Chem. Soc.* **2004**, *126*, 14964.
- (19) Li, D.; Xia, Y. N. *Adv. Mater.* **2004**, *16*, 1151.
- (20) Kloppenburg, L.; Jones, D.; Bunz, U. H. F. *Macromolecules* **1999**, *32*, 4194.
- (21) Wilson, J. N.; Bangcuyo, C. G.; Erdogan, B.; Myrick, M. L.; Bunz, U. H. F. *Macromolecules* **2003**, *36*, 1426.
- (22) (a) Song, L.; Bly, R. K.; Wilson, J. N.; Bakbak, S.; Park, J. O.; Srinivasarao, M.; Bunz, U. H. F. *Adv. Mater.* **2004**, *16*, 115. (b) Bunz, U. H. F. *Adv. Mater.* **2006**, *18*, 973. (c) Srinivasarao, M.; Collings, D.; Philips, A.; Patel, S. *Science* **2001**, *292*, 79.
- (23) McConnell, W. P.; Novak, J. P.; Brousseau, L. C.; Fuierer, R. R.; Tenent, R. C.; Feldheim, D. L. *J. Phys. Chem. B* **2000**, *104*, 8925.
- (24) Bunz, U. H. F.; Enkelmann, V.; Kloppenburg, L.; Jones, D.; Shimizu, K. D.; Claridge, J. B.; zur Loye, H.-C.; Lieser, G. *Chem. Mater.* **1999**, *11*, 1416.
- (25) (a) Martin, C. R. *Science* **1994**, *266*, 1961. (b) Martin, C. R. *Chem. Mater.* **1996**, *8*, 1739. (c) Martin, C. R. *Acc. Chem. Res.* **1995**, *28*, 61.
- (26) (a) Wang, Y. Q.; Erdogan, B.; Wilson, J. N.; Bunz, U. H. F. *Chem. Commun.* **2003**, 1624. (b) The orientation of the polyester-containing side chains on the benzene ring is not clear, the shown representation was chosen for convenience and does not imply any stereochemical preference or head to tail orientation of two neighboring polyester-carrying benzene rings. We would speculate that these polymers **9–12** and **5** are regiorandom.
- (27) (a) Perahia, D.; Traiphol, R.; Bunz, U. H. F. *J. Chem. Phys.* **2002**, *117*, 1827. (b) Perahia, D.; Traiphol, R.; Bunz, U. H. F. *Macromolecules* **2001**, *34*, 151. (c) Jiang, Y.; Perahia, D.; Wang, Y.; Bunz, U. H. F. *Macromolecules* **2006**, *39*, 4941.
- (28) Deotare, P. B.; Kameoka, J. *Nanotechnology* **2006**, *17*, 1380.
- (29) (a) Cassie, A. B. D.; Baxter, S. *Trans. Faraday Soc.* **1944**, *40*, 546. (b) Cassie, A. B. D. *Discussions Faraday Soc.* **1948**, *3*, 11.
- (30) McCann, J. T.; Marquez, M.; Xia, Y. *J. Am. Chem. Soc.* **2006**, *128*, 1436.
- (31) Bognitzki, M.; Hou, H.; Ishaque, M.; Frese, T.; Hellwig, M.; Schwarte, C.; Schaper, A.; Wendorff, J. H.; Greiner, A. *Adv. Mater.* **2000**, *12*, 637.
- (32) (a) Lakowicz, J. R. *Principles of fluorescence spectroscopy*, 2nd ed.; Springer Science: Heidelberg, Germany, 2004. (b) *A Guide to Recording Fluorescence Quantum Yields*; Horiba Jobin Yvon Ltd.: U.K., 200X. Available online: <http://www.jobinyvon.co.uk/ukdivisions/Fluorescence/plqy.htm>.

MA062801D